Article

Inhibition of Amyloid # Protein Fibrillation by Polymeric Nanoparticles

Celia Cabaleiro-Lago, Fiona Quinlan-Pluck, Iseult Lynch, Stina Lindman, Aedin M. Minogue, Eva Thulin, Dominic M. Walsh, Kenneth A. Dawson, and Sara Linse

J. Am. Chem. Soc., **2008**, 130 (46), 15437-15443 • DOI: 10.1021/ja8041806 • Publication Date (Web): 28 October 2008

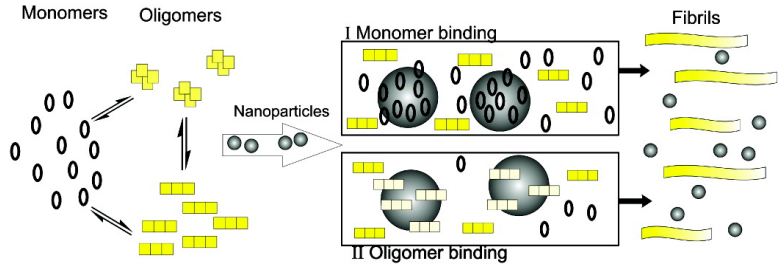

More About This Article

Additional resources and features associated with this article are available within the HTML version:

- Supporting Information
- Access to high resolution figures
- Links to articles and content related to this article
- Copyright permission to reproduce figures and/or text from this article

View the Full Text HTML

J|A|C|S
ARTICLES

Published on Web 10/28/2008

Inhibition of Amyloid β Protein Fibrillation by Polymeric Nanoparticles

Celia Cabaleiro-Lago,[†,§] Fiona Quinlan-Pluck,[†,§] Iseult Lynch,[†] Stina Lindman,[‡] Aedin M. Minogue,[§] Eva Thulin,[‡] Dominic M. Walsh,[§] Kenneth A. Dawson,[*,†] and Sara Linse[‡]

Centre for BioNano Interactions, School of Chemistry and Chemical Biology, University College Dublin, Belfield, Dublin 4, Ireland, Department of Biophysical Chemistry, Lund University, P.O. Box 124, 22100 Lund, Sweden, and Laboratory for Neurodegenerative Research, UCD Conway Institute for Biomolecular and Biomedical Research, University College Dublin, Belfield, Dublin 4, Ireland

Received June 3, 2008; E-mail: kenneth@fiachra.ucd.ie

Abstract: Copolymeric NiPAM:BAM nanoparticles of varying hydrophobicity were found to retard fibrillation of the Alzheimer's disease-associated amyloid β protein (Aβ). We found that these nanoparticles affect mainly the nucleation step of Aβ fibrillation. The elongation step is largely unaffected by the particles, and once the Aβ is nucleated, the fibrillation process occurs with the same rate as in the absence of nanoparticles. The extension of the lag phase for fibrillation of Aβ is strongly dependent on both the amount and surface character of the nanoparticles. Surface plasmon resonance studies show that Aβ binds to the nanoparticles and provide rate and equilibrium constants for the interaction. Numerical analysis of the kinetic data for fibrillation suggests that binding of monomeric Aβ and prefibrillar oligomers to the nanoparticles prevents fibrillation. Moreover, we find that fibrillation of Aβ initiated in the absence of nanoparticles can be reversed by addition of nanoparticles up to a particular time point before mature fibrils appear.

Introduction

The ability of proteins to form amyloid fibrils seems to be largely sequence-independent, and many proteins can form structures with characteristic cross-β stacking perpendicular to the long axis of the fiber.[1−3] While the molecular events behind the processes leading from native to fibrillar states remain elusive, data accumulated from many studies suggest that fibrillation involves a number of intermediate oligomeric states of different association numbers and structures.[4,5] The use of agents that interfere with these processes and/or allow for the isolation of intermediate species may help elucidate the molecular mechanism of fibril formation. Such strategies also have therapeutic potential for the treatment of amyloidosis.

We recently identified copolymeric nanoparticles as agents that accelerate the fibrillation of β2microglobulin (β2m).[6] Specifically, we found that the presence of nanoparticles leads to a shortening of the lag phase for nucleation of the fibrillation process. The likely role of the nanoparticles in this process is binding of β2m, which increases the local concentration and the likelihood of formation of a critical nucleus for fibrillation.[6] Depending on the relative affinity of nanoparticles for protein monomers, unfolded monomers, oligomers, critical nuclei, and other prefibrillar states, the influence of nanoparticles on protein fibrillation kinetics is likely to be protein-dependent. Quite different effects may also be anticipated if the protein species are bound in a similar conformation as in solution or if the binding process alters the conformation of the protein or causes local or global unfolding. Thus, to further our understanding of protein fibrillation processes and how these are perturbed by the presence of nanoparticles, it is necessary to collect large amounts of well-controlled data in a protein- and particle-dependent manner.

In the present study, we have investigated the effect of copolymeric *N*-isopropylacrylamide: *N-tert*-butylacrylamide (NiPAM:BAM) nanoparticles having a nominal size of 40 nm on the fibrillation of amyloid β protein (Aβ). Previous studies in the literature regarding Aβ and nanoparticles have focused on detection and diagnosis[7,8] or targeting and destruction[9,10] of amyloid aggregates, and only a few papers have investigated

[†] School of Chemistry and Chemical Biology, University College Dublin.
[‡] Department of Biophysical Chemistry, Lund University.
[§] UCD Conway Institute for Biomolecular and Biomedical Research, University College Dublin.

(1) Kelly, J. W. *Structure* **1997**, *5*, 595–600.
(2) Sunde, M.; Blake, C. *Adv. Protein Chem.* **1997**, *50*, 123–159.
(3) Teplow, D. B. *Amyloid* **1998**, *5*, 121–142.
(4) Chiti, F.; Dobson, C. M. *Annu. Rev. Biochem.* **2006**, *75*, 333–366.
(5) Stefani, M.; Dobson, C. M. *J. Mol. Med.* **2003**, *81*, 678–699.
(6) Linse, S.; Cabaleiro-Lago, C.; Xue, W. F.; Lynch, I.; Lindman, S.; Thulin, E.; Radford, S. E.; Dawson, K. A *Proc. Natl. Acad. Sci. U.S.A.* **2007**, *104*, 8691–8696.
(7) Choi, J. S.; Choi, H. J.; Jung, D. C.; Lee, J. H.; Cheon, J. *Chem. Commun.* **2008**, 2197–2199.
(8) Haes, A. J.; Hall, W. P.; Chang, L.; Klein, W. L.; Van Duyne, R. P. *Nano Lett.* **2004**, *4*, 1029–1034.
(9) Bastus, N. G.; Kogan, M. J.; Amigo, R.; Grillo-Bosch, D.; Araya, E.; Turiel, A.; Labarta, A.; Giralt, E.; Puntes, V. F. *Mater. Sci. Eng., C* **2007**, *27*, 1236–1240.
(10) Olmedo, I.; Araya, E.; Sanz, F.; Medina, E.; Arbiol, J.; Toledo, P.; Alvarez-Lueje, A.; Giralt, E.; Kogan, M. J. *Bioconjugate Chem.* **2008**, *19*, 1154–1163.

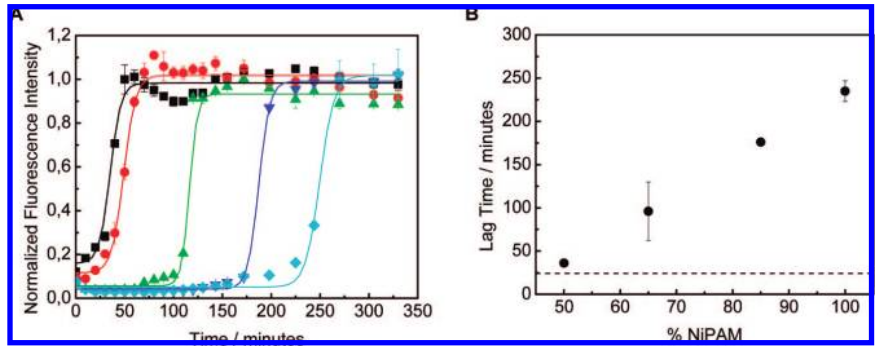

Figure 1. (A) Fibrillation kinetics of Aβ(M1−40) at 37 °C monitored by the temporal development of thioflavin T binding in the absence (■) and in the presence of 50:50 (●), 65:35 (▲), 85:15 (▼), and 100:0 (◆) NiPAM:BAM polymeric particles having a diameter of 40 nm. Each sample contained 10 μM Aβ(M1−40), 200 μM ThT, and 5 μg/mL particles in 10 mM sodium phosphate buffer, 0.02% NaN_3, pH 7.4. Lines indicate best fits of eq 1 to the data. Averages and standard errors of the mean of six replicates are shown. (B) Lag times of fibrillation vs the percentage of NiPAM monomer in the NiPAM:BAM particles. Error bars indicate the standard error of the mean. The dotted line indicates the lag time in the absence of particles (from fitting of eq 1). It should be noted that slightly different plateau values were found, depending on the experimental conditions. It is believed that the ThT signal may depend on the microscopic organization and division of the fibrils. We have not yet attempted to differentiate between those effects, and therefore, for clearer comparison, the curves have been normalized to the maximum plateau value for each data set.

in detail the effect of nanoparticles on Aβ fibrillation.[11−13] The NiPAM:BAM particles, with controlled size and purity, allow us to systematically change the particle properties by changing the monomer ratio[14] and thereby to analyze the possible consequences of surface properties on amyloid fibrillation. This kind of particle has previously been tested as a drug delivery system[15−17] because of its thermoresponsive characteristics and biocompatibility.[15,18] The nanoparticles used in this study were characterized under several reference conditions (Table S1 in the Supporting Information), which in principle enables reproduction of the results by ensuring that all of the experiments start with the same nanoparticle sizes and surfaces.

However, the question of the structures of actual dispersions of nanoparticles, proteins, and evolving fibrils is much more complex and demanding and certainly involves a degree of progressive aggregation of the nanoparticles under the experimental conditions (i.e., such a dispersion is a nonequilibrium system). If one wishes to work with nanoparticle−protein interactions of this type, then one always, by definition, must work with an intrinsically unstable system. The best that can be achieved is to limit the degree of instability by working in relevant concentration regimes and to ensure that the consequences of any slow instabilities are at least reproducible by initiating the experiments at the same time and in a reproducible manner. We have taken both of these steps in the research presented here.

Aβ is the principal protein component of the amyloid plaques that characterize Alzheimer's disease, and extensive data support a central role for Aβ in the disease process. Until relatively recently, it was assumed that Aβ had to be assembled into amyloid fibrils to exert its cytotoxic effects. However, it is now clear that prefibrillar, diffusible assemblies of Aβ are also deleterious.[19] We find that the presence of copolymeric nanoparticles strongly retards fibrillation of Aβ in a manner that depends on the amount and surface character of the particles. Moreover, we find that fibrillation initiated in the absence of nanoparticles can, up to a certain time point, be reversed, thus preventing amyloid fibril formation. This phenomenon was observed using either synthetic Aβ(1−40) or Aβ(1−42) (Figure S2 in the Supporting Information) or recombinant Aβ(M1−40) bearing an N-terminal methionine.

Results

Kinetics of Aβ(M1−40) Fibrillation. The formation of amyloid aggregates was studied in the absence and presence of copolymeric particles using a continuous thioflavin T (ThT) binding assay. Interaction of amyloid fibrils and protofibrils with ThT causes a red shift in its excitation spectrum,[20] and ThT fluorescence is therefore a measure of fibrillogenesis. Fibrillation of Aβ appears to be highly cooperative, reminiscent of first-order phase transitions (e.g., "crystallization"),[21−23] and the fibrillation kinetics measured here for 10 μM Aβ(M1−40) exhibits characteristics of a typical nucleation and growth process (Figure 1). The time course of fibrillogenesis includes a lag phase (during which no ThT binding assemblies are detectable) followed by a rapid exponential growth (elongation) of fibrils. This lag time is assumed to be the activation time required for the formation of a "critical" nucleus, which likely requires unfavorable monomeric protein conformational rearrangements and improbable alignments into protein clusters. However, assuming the fibril has a lower free energy, sufficiently large nuclei will be preferentially stable and unlikely to revert to monomeric proteins. Then, elongation of fibrils occurs rapidly by association of monomers or oligomers to the

(11) Kim, J. E.; Lee, M. *Biochem. Biophys. Res. Commun.* **2003**, *303*, 576–579.
(12) Yokoyama, K.; Welchons, D. R. *Nanotechnology* **2007**, *18*, 105101.
(13) Ikeda, K.; Okada, T.; Sawada, S.; Akiyoshi, K.; Matsuzaki, K. *FEBS Lett.* **2006**, *580*, 6587–6595.
(14) Yi, Y. D.; Bae, Y. C. *J. Appl. Polym. Sci.* **1998**, *67*, 2087–2092.
(15) Sershen, S. R.; Westcott, S. L.; Halas, N. J.; West, J. L. *J. Biomed. Mater. Res.* **2000**, *51*, 293–298.
(16) Salvati, A.; Soderman, O.; Lynch, I. *J. Phys. Chem. B* **2007**, *111*, 7367–7376.
(17) Lynch, I.; de Gregorio, P.; Dawson, K. A. *J. Phys. Chem. B* **2005**, *109*, 6257–6261.
(18) Saunders, B. R.; Vincent, B. *Adv. Colloid Interface Sci.* **1999**, *80*, 1–25.
(19) Walsh, D. M.; Selkoe, D. J. *Neuron* **2004**, *44*, 181–193.
(20) Levine, H. *Amyloid* **1995**, *2*, 1–6.
(21) Jarrett, J. T.; Berger, E. P.; Lansbury, P. T. *Biochemistry* **1993**, *32*, 4693–4697.
(22) Naiki, H.; Nakakuki, K. *Lab. Invest.* **1996**, *74*, 374–383.
(23) Gunton, J. D. *J. Stat. Phys.* **1999**, *95*, 903–923.

Table 1. Values of $t_{1/2}$, Lag Time, and Apparent Aggregation Constant (k) Obtained for the Experiment Shown in Figure 1[a]

	$t_{1/2}$ (min)	lag time (min)	k (min^{-1})
no particles	37 ± 1	30 ± 4	0.28 ± 0.03
50:50	49 ± 1	36 ± 4	0.16 ± 0.03
65:35	102 ± 10	96 ± 34	0.34 ± 0.12
85:15	186 ± 2	176 ± 4	0.19 ± 0.02
100:0[b]	250 ± 5	235 ± 12	0.13 ± 0.03

[a] Reported values are averages of the results obtained from fitting the empirical eq 1 to the experimental data for each replicate of the experiment shown in Figure 1 using particles at 5 μg/mL (45 pM) and Aβ(M1−40) at 10 μM. Errors indicate the standard error of the mean. [b] In the 100:0 case, one experimental point was removed from the analysis because of its large deviation from the observed trend.

nucleus and growing fibrils.[4,24] The presence of copolymeric nanoparticles leads to a significant increase in the lag phase of Aβ(M1−40) fibrillation but does not completely inhibit fibril formation (Figure 1). Thus it would appear that the particles act to reduce the rate of nucleation, but once critical nuclei are formed, elongation is essentially unaffected by the presence of the nanoparticles.

The effects of nanoparticles on the two processes, nucleation and elongation, may be codified in terms of kinetic parameters relevant to these subprocesses that can be obtained by fitting the data. Traditionally, amyloid aggregation kinetics has been described by a sigmoidal curve defined by a lag phase, subsequent growth, and a final equilibrium phase.[22,25−27] Independent of the type of amyloid protein, experimental data are fitted reasonably well by such a sigmoidal curve (eq 1):[26]

$$y = y_0 + \frac{y_{max} - y_0}{1 + e^{-(t - t_{1/2})k}} \quad (1)$$

where y is the fluorescence intensity at time t, y_0 and y_{max} are the initial and maximum fluorescence intensities, respectively, $t_{1/2}$ is the time required to reach half the maximum fluorescence intensity (halfway from nuclei to fibrils), and k is the apparent first-order aggregation constant. The lag time is defined as the time at which the tangent at the point of the maximum fibrillation rate intersects the abscissa, which is given by eq 2:

$$\text{lag time} = t_{1/2} - \frac{2}{k} \quad (2)$$

Interestingly, the sigmoidal curve given by eq 1 is close to that expected from conventional kinetics studies of phase transitions. By analogy, we surmise that the smoothing of the (expected) very sharp kinetic transition likely stems from an anomalously large distribution of critical nucleation events, possibly a result of the sequence-specific assembly processes required to form critical nuclei.

All four nanoparticles studied here at a concentration of 5 μg/mL (45 pM) lead to a significant extension of the lag phase but have little effect on the elongation phase (Table 1). In the most extreme case (100:0 NiPAM:BAM) we have an ∼7 fold increase in the length of the lag phase. Thus, in the absence of particles, fibril formation is completed long before nucleation has even occurred in samples where high-NiPAM-content particles are present. The values of the apparent aggregation constant k indicate that the elongation process is not significantly affected by the addition of nanoparticles. Furthermore, the lag times clearly depend on the chemical

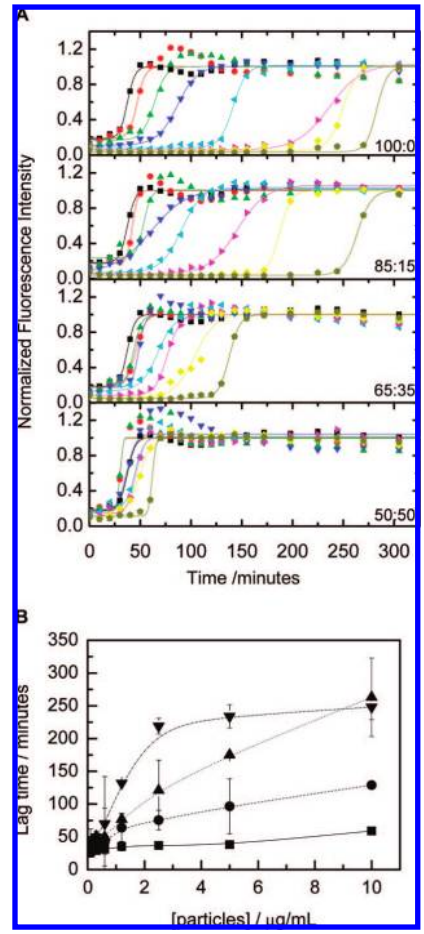

Figure 2. (A) Fibrillation kinetics of Aβ(M1−40) at 37 °C monitored by the temporal development of thioflavin T fluorescence for four different nanoparticles formed using differing NiPAM:BAM ratios (given in the graph labels). For each particle type, the concentration was varied from 0 to 10 μg/mL: (■) 0, (●) 0.1, (▲) 0.3, (▼) 0.6, (left-pointing triangles) 1.2, (right-pointing triangles) 2.5, (◆) 5, and (pentagons) 10 μg/mL. Each sample contained 10 μM Aβ(M1−40) and 200 μM ThT in 10 mM sodium phosphate buffer, 0.02% NaN_3, pH 7.4. Lines indicate fits of eq 1. (B) Lag times as functions of nanoparticle concentration, obtained by fitting eq 1 to the experimental data for the different particle compositions: (■) 50:50, (●) 65:35, (▲) 85:15, and (▼) 100:0 NiPAM:BAM copolymer particles. Lines are guides for the eye, and error bars indicate the standard error of the mean.

composition of the particles (Figure 1b). As the amount of NiPAM in the nanoparticle composition increases, the lag time for fibrillation increases. The surface properties of these particles are markedly determined by the ratio between the two monomers, which have different hydrophobicities, and a correlation between particle properties and kinetic effects is therefore expected.

The fibrillation kinetics of 10 μM Aβ(M1−40) were studied as a function of nanoparticle concentration in the range 0.1−10 μg/mL (0.9−90 pM) (Figure 2), corresponding to a 7×10^4 to 7×10^6-fold molar excess of Aβ(M1−40). The inhibitory effect (Figure 2) is concentration-dependent, and the amount of particles required to observe a significant effect on the lag phase increases as the amount of BAM in the particles increases. For 50:50 NiPAM:BAM, addition of particles at a concentration of 10 μg/mL is needed in order to see a significant effect. In contrast, 100:0 NiPAM:BAM particles produce a significant extension of the lag phase at particle concentrations as low as 0.1 μg/mL, while the highest concentration (10 μg/mL) leads

(24) Jarrett, J. T.; Lansbury, P. T. *Biochemistry* **1992**, *31*, 12345–12352.

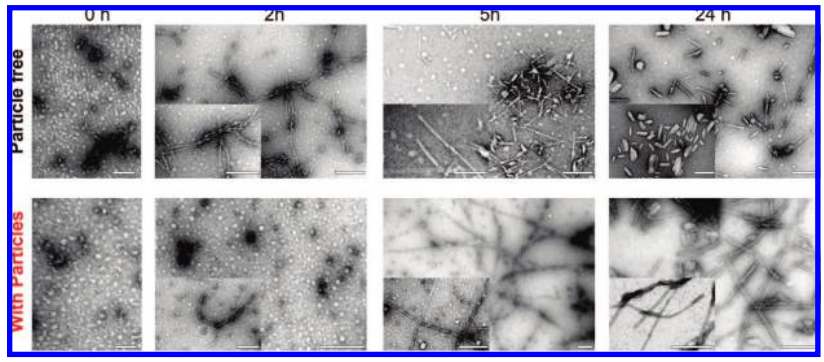

Figure 3. TEM images of fibrillation time courses in the absence and presence of 40 nm diameter 85:15 NiPAM:BAM nanoparticles at 30 μg/mL at a peptide concentration of 25 μM. The top row shows images in the absence of particles, and the bottom row includes images of samples with nanoparticles obtained after 0, 2, 5, and 24 h of the fibrillation reaction. The scale bar indicates 200 nm. Illustrative ThT evolution for these experimental conditions can be found in Figure S3 in the Supporting Information, where ThT was added to the TEM solutions for the fluorescence assay. Because of the low concentration and presumably low binding to the TEM grid, nanoparticles were not observed in the TEM specimens prepared. Higher particle concentrations are required in order to see the particles in the protein solution (see Figure S4 in the Supporting Information).

to a 10-fold increase in lag time. Our results thus show that the pure NiPAM particles have the greatest ability to prevent Aβ(M1−40) fibrillation (Table 1). The inhibition of Aβ(M1−40) fibrillation via lengthening of the lag phase is dependent on both the concentration and surface properties of the copolymeric nanoparticles. Particle aggregation was found to be negligible over the time course of the experiment over most of the concentration range studied (0.0001−0.01 mg/mL) both in the absence and in the presence of Aβ (see the Supporting Information).

Recent data indicate that other nonfibrillar assemblies may also bind ThT,[28] and it is well-known that the presence of ThT in the protein solution influences the fibrillation process. To address these issues, fibril formation was confirmed by electron microscopy (Figure 3) and a parallel TEM and ThT assay (Figure S3 in the Supporting Information), indicating good agreement between the two methods in terms of reporting on the fibrillation process. After 2 h of reaction, fibrils are observed only in the sample without nanoparticles. The fibrils are 50−800 nm long, 6−10 nm wide, and nonbranched.[29−31] After 5 h, fibril networks are observed in both samples, although the fibrils are shorter in the absence of nanoparticles (0.5−600 nm) than in their presence (0.4−2 μm). Moreover, the particle-free sample presents thick segments formed by association of very short fibrils (~50 nm) that are not observed in the sample with particles. After 24 h, both samples show similar features, namely, a coexistence of short, rigid fibrils and sheets of laterally associated fibrils. The shortening of the fibrils as the reaction develops might be explained by fracture of long fibrils caused by shaking followed by lateral association into short sheet-like structures. If this is the case, it could be expected that by 36 h the fibrils in the presence of the nanoparticles would also be short and bundled.

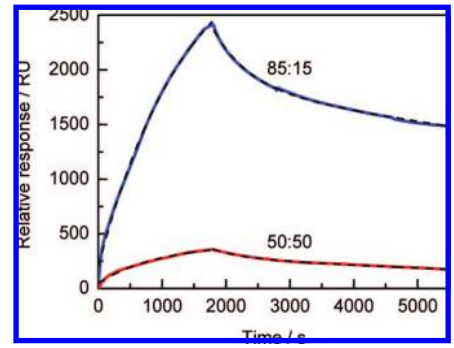

Figure 4. SPR data for Aβ(M1−40) binding to 40 nm (blue) 85:15 and (red) 50:50 NiPAM:BAM particles together with fitted curves (dashed lines) obtained using eqs S1 and S2 in the Supporting Information. Aβ(M1−40) was injected over the nanoparticle-coated surfaces in 10 mM Tris/HCl buffer with 150 mM NaCl, 3 mM EDTA, and 0.005% Tween 20 for 1800 s followed by continuous flow of the same buffer (the first 3900 s are shown).

Binding of Aβ(M1−40) to Nanoparticles. The interaction of Aβ(M1−40) with the copolymeric nanoparticles was studied using surface plasmon resonance (SPR) with 50:50 or 85:15 NiPAM:BAM particles linked to gold via a thiol group.[32] The sensorgrams (Figure 4) clearly show that Aβ(M1−40) binds to both types of nanoparticle and dissociates slowly, but the amplitude, and thus the number of bound peptides per particle, is higher for 85:15 than for 50:50 NiPAM:BAM particles. The rate constants were estimated from computer fits to the sensorgram data. As shown in Figure 4, the association phase data for both particles are well-fitted assuming a single kinetic process (eq S2 in the Supporting Information), while acceptable fitting of the dissociation phase data requires at least two kinetic processes (a sum of two exponential decays, eq S1 in the Supporting Information). The dissociation rate constants in the case of Aβ(M1−40) interacting with 85:15 NiPAM:BAM nanoparticles were $k^{off1} = 6 \times 10^{-5}$ s^{-1} and $k^{off2} = 2 \times 10^{-3}$ s^{-1}, and the amplitude of the slow phase represented 78% of the total amplitude. The value for k^{off1} was therefore used to fit the association phase data, and we obtained $k^{on} = 63$ M^{-1} s^{-1}.

(25) Lee, C. C.; Nayak, A.; Sethuraman, A.; Belfort, G.; McRae, G. J. *Biophys. J.* **2007**, *92*, 3448–3458.
(26) Nielsen, L.; Khurana, R.; Coats, A.; Frokjaer, S.; Brange, J.; Vyas, S.; Uversky, V. N.; Fink, A. L. *Biochemistry* **2001**, *40*, 6036–6046.
(27) Necula, M.; Breydo, L.; Milton, S.; Kayed, R.; van der Veer, W. E.; Tone, P.; Glabe, C. G. *Biochemistry* **2007**, *46*, 8850–8860.
(28) Walsh, D. M.; Hartley, D. M.; Kusumoto, Y.; Fezoui, Y.; Condron, M. M.; Lomakin, A.; Benedek, G. B.; Selkoe, D. J.; Teplow, D. B. *J. Biol. Chem.* **1999**, *274*, 25945–25952.
(29) Goldsbury, C.; Frey, P.; Olivieri, V.; Aebi, U.; Muller, S. A. *J. Mol. Biol.* **2005**, *352*, 282–298.
(30) Goldsbury, C. S.; Wirtz, S.; Muller, S. A.; Sunderji, S.; Wicki, P.; Aebi, U.; Frey, P. *J. Struct. Biol.* **2000**, *130*, 217–231.
(31) Jimenez, J. L.; Nettleton, E. J.; Bouchard, M.; Robinson, C. V.; Dobson, C. M.; Saibil, H. R. *Proc. Natl. Acad. Sci. U.S.A.* **2002**, *99*, 9196–9201.
(32) Cedervall, T.; Lynch, I.; Lindman, S.; Berggard, T.; Thulin, E.; Nilsson, H.; Dawson, K. A.; Linse, S. *Proc. Natl. Acad. Sci. U.S.A.* **2007**, *104*, 2050–2055.

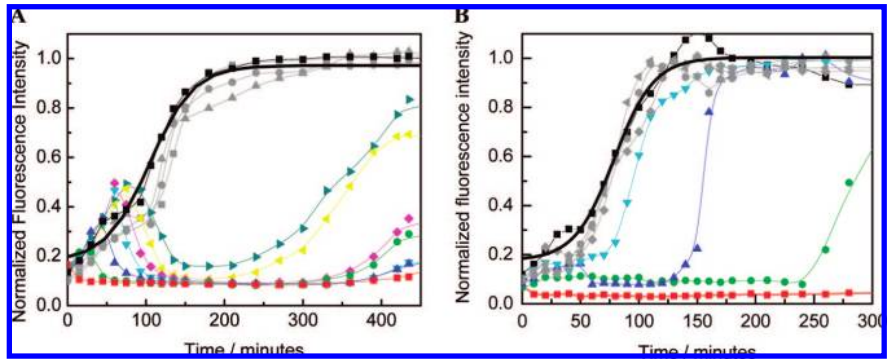

Figure 5. (A) Fibrillation kinetics of Aβ(M1−40) at 37 °C monitored by measuring the increase in thioflavin T fluorescence when 6 μM Aβ(M1−40) was incubated with 200 μM ThT in 10 mM phosphate buffer, 0.02% NaN_3, pH 7.4, in the presence or absence of 10 μg/mL 85:15 NiPAM:BAM nanoparticles. Particles were added every 15 min from 0 to 120 min and then at 30 min intervals up to 330 min. Colored curves indicate time points where the addition of particles has a significant effect, whereas gray curves indicate time points were the addition of particles had no effect: (■) 0, (●) 15, (▲) 30, (▼) 45, (◆) 60, (left-pointing triangles) 75, (right-pointing triangles) 90 min, and (gray) 90−195 min. The control reaction without added nanoparticles is shown in black. (B) Fibrillation kinetics in the presence or absence of 10 μg/mL 65:35 NiPAM:BAM nanoparticles. Particles were added every 15 min from 0 to 120 min and then at 30 min intervals up to 330 min: (■) 0, (●) 15, (▲) 30, (▼) 45 min, and (gray) >60 min. The control reaction without added nanoparticles is shown in black. The heavy black curve is the fit of eq 1 to the experimental data in the absence of nanoparticles.

The equilibrium association constant was estimated from the ratio k^{on}/k^{off1} to be $K_A = 1 \times 10^6$ M^{-1}. For Aβ(M1−40) interacting with 50:50 NiPAM:BAM nanoparticles, we obtained $k^{off1} = 1.3 \times 10^{-4}$ s^{-1} (79% of the total amplitude), $k^{off2} = 2 \times 10^{-3}$ s^{-1}, $k^{on} = 93$ M^{-1} s^{-1}, and $K_A = 7 \times 10^5$ M^{-1}. The affinity of Aβ(M1−40) for the two nanoparticles thus seems to be quite similar within the error limits of the experiments.

The interaction of Aβ with the copolymeric nanoparticles (using 50:50 and 100:0 NiPAM:BAM particles) was also studied using isothermal titration calorimetry. Several individual experiments were performed and compared to parallel experiments with Aβ(M1−40) injected into buffer without nanoparticles. No reaction heats were observed, implying that Aβ binding to the copolymeric nanoparticles is entropy-driven ($\Delta H = 0$), as was also observed for several other proteins.[33]

Influence of Nanoparticle Addition Time. On the basis of an understanding of the relationship between the kinetics curves and the mechanism of nucleation and the growth kinetics, one can seek more insight into the mechanism of action of the polymeric nanoparticles using experiments performed with addition of nanoparticles at different times. In a typical experiment, after the fibrillation reaction starts, particles are added at selected times and the kinetic evolution monitored by ThT fluorescence. Figure 5a shows examples of data obtained for the 85:15 NiPAM:BAM nanoparticles. In the kinetic traces without nanoparticles we see a short lag phase, then an early phase of ThT fluorescence increase, and then a leveling off before the final increase to reach a plateau value. This early ThT-reactive species may be the key to explaining the mechanism of nanoparticle action. Our data show that we can temporarily reverse the process and prevent fibrillation if we add nanoparticles up to and during this first phase of ThT fluorescence increase but not after mature fibrils have started to form.

When 85:15 NiPAM:BAM particles are added at $t = 0$ (before the fibrillation starts), there is no increase of fluorescence signal and no formation of ThT-reactive aggregates or fibrils during a time frame longer than 5 times the lag phase for the control experiment. However, if particles are injected after the fluorescence intensity has started to increase (ThT-reactive aggregates are formed), the fluorescence intensity decreases in response to the nanoparticles. This effect is only observed for nanoparticles added at the early stages of the fibrillation curve. On the basis of a general understanding of phase-transition kinetics, the regime after which nanoparticle addition has no significant effect is consistent with the critical nucleation regime. Beyond this, it is impossible to stop fibrillation. The decrease of fluorescence intensity upon addition of 85:15 NiPAM:BAM nanoparticles is intriguing. It may represent a shift of the quasi-equilibrium state toward monomer (according to the classical Le Châtelier's principle), as removal of monomeric proteins leads to lower concentration and loss of the more kinetically advanced species, requiring additional lag time to produce more of this species. Alternatively, it may arise from quenching of the fluorescence signal of ThT bound to oligomers (likely critical and subcritical nuclei) that adsorb onto the particle surface, blocking key epitopes and thereby inhibiting the primary route of fibril growth.

Addition of 65:35 NiPAM:BAM particles up to a certain point slows down the nucleation step, but after this point, elongation proceeds as in absence of particles (Figure 5b). In contrast to the case of the 85:15 particles, the decrease in the ThT signal after particle addition is minor (with the exception of particles added at $t = 0$), showing a stable value until fibrillation starts and the fluorescence intensity increases toward a final plateau.

The ability to revert an ongoing aggregation/fibrillation process is correlated with the particle composition. The time at which addition of particles no longer influences the fibrillation process decreases as the amount of BAM increases. For 100:0 (data not shown), 85:15, and 65:35 NiPAM:BAM, the average limit times are 75 ± 21, 67 ± 15, and 42 ± 4 min, respectively. The 50:50 NiPAM:BAM particles have a somewhat limited inhibitory effect only if they are added before 18 ± 8 min, at which time we suppose critical nuclei have appeared (data not shown).

Discussion

Our results imply that the nucleation process of Aβ is strongly disturbed by the presence of copolymeric nanoparticles and that the perturbation depends on the surface properties of the particles. We are able to narrow the options for the mechanism but cannot yet determine it fully.

(33) Lindman, S.; Lynch, I.; Thulin, E.; Nilsson, H.; Dawson, K. A.; Linse, S. *Nano Lett.* **2007**, *7*, 914–920.

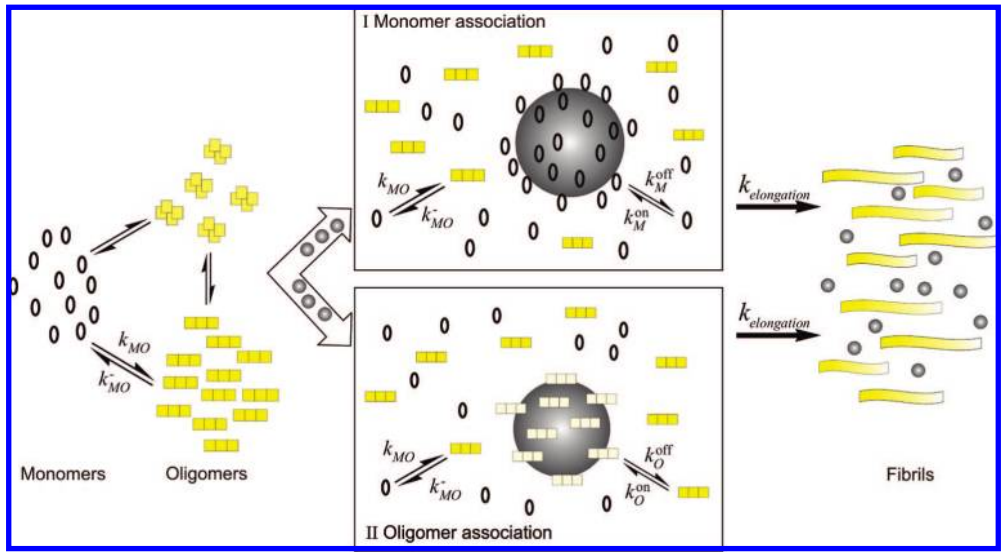

Figure 6. Schematic representation of the possible modes of interaction between copolymeric nanoparticles and Aβ. Gray spheres indicate nanoparticles, and yellow clusters indicate structured and unstructured oligomers. The constants k_j shown in the scheme represent the rate constants of the different processes considered in our model and are included for indicative purposes only.

Fibrillation may be loosely considered to be a four-state process involving quasi-static equilibria between monomers and subcritical and critical nuclei followed by an essentially irreversible conversion of critical nuclei to mature fibrils.[5] Within this framework, the fibrillation rate can be modified by disturbing the first and second quasi-equilibria in a variety of manners. While our data clearly show that Aβ(M1−40) binds to the particles, we cannot distinguish between binding of monomeric and oligomeric forms. Thus, two natural models for the effects of nanoparticles present themselves (Figure 6):

I. Binding of Aβ monomer: Upon addition of the particles, monomer is bound, inhibiting fibrillation simply by decreasing the amount of monomer in solution. Trapping of monomers disturbs the monomer−oligomer equilibrium, which must be re-established by dissociation of early aggregates. At some point in this stochastic process, however, the critical nuclei form, and rapid growth into fibrils follows.

II. Binding of Aβ oligomer: Particles bind oligomers of Aβ, leading to depletion of sub- and near-critical oligomers. Binding would imply a reduction of oligomer concentration in solution, affecting the nucleation step. Moreover, those oligomers that do bind are unlikely to lead to fibrillation, since the particle would hinder the elongation process by blocking sites for monomer addition on the aggregates.

It should be noted that either of these mechanisms is capable of causing a reduction in the number of oligomers that bind ThT and thereby a reduction of (or, at least, no further increase of) ThT fluorescence. Both models are broadly compatible with the data we have presented so far.

The association rate is governed by the association rate constant and the concentrations of the interacting species. The SPR experiments were therefore set up under conditions similar to those used in the fibrillation experiments. Under these conditions, saturation is reached over a time scale of 30−90 min (Figure 4), which is also the characteristic time required for loss of (or inhibition of further) fibril-related fluorescence. This supports a key role for protein binding in the inhibition of fibrillation by the nanoparticles, but does no more than this.

Several scenarios suggest themselves at this point. Adsorption of high amounts of protein onto particle surfaces implies a high local concentration on the surface. In a previous example that we have studied, the protein β2m,[6] the shortening of the lag phase for fibrillation was interpreted as an adsorption-related enhanced formation of critical nuclei. Observation of the opposite effect for Aβ[11] might suggest that tight interactions between the nanoparticle surface and Aβ(M1−40) monomers or oligomers lead to unfavorable conditions for fibril growth through blocking of binding sites for the addition of new monomers. This would lead to depletion of the sub- and near-critical oligomers and to partial blockage of the kinetic pathway until the particle surface is saturated and new nuclei can be grown. Another possibility is that the adsorption of monomer lowers the concentration of free protein, shifting the equilibrium away from fibrillation.

Another important difference between the two cases is that β2m is a protein, although partially unfolded at low pH, whereas Aβ is a relatively unstructured peptide. For β2m, the intraprotein contacts are somewhat internalized and need to be presented appropriately for the protein to fibrillate. This process may be facilitated in early oligomers formed on the particle surface, whereas the more unfolded Aβ has a lower kinetic barrier to fibrillation and is instead hindered from fibrillation by being captured on the surface.

Whatever the detailed kinetic mechanism, the distinctive role of NiPAM is striking. Different noncovalent interactions may govern the association of proteins with solid surfaces.[34] Previous studies on flat surfaces indicate that Aβ monomers and seeds bind preferentially to hydrophobic and positively charged surfaces,[35−37] preventing or hindering the fibrillation process.[35] The amphiphatic character of the peptide, with a highly hydrophobic C-terminal portion, favors hydrophobic interactions with the hydrophobic copolymeric particles. The particle composition determines its hydrophobic character, as confirmed

(34) Lee, S. H.; Ruckenstein, E. *J. Colloid Interface Sci.* **1988**, *125*, 365–379.
(35) Ban, T.; Morigaki, K.; Yagi, H.; Kawasaki, T.; Kobayashi, A.; Yuba, S.; Naiki, H.; Goto, Y. *J. Biol. Chem.* **2006**, *281*, 33677–33683.
(36) Kowalewski, T.; Holtzman, D. M. *Proc. Natl. Acad. Sci. U.S.A.* **1999**, *96*, 3688–3693.
(37) Rocha, S.; Krastev, R.; Thunemann, A. F.; Pereira, M. C.; Mohwald, H.; Brezesinski, G. *ChemPhysChem* **2005**, *6*, 2527–2534.

Table 2. Values of the Pyrene I_1/I_3 Ratio for Water and Nanoparticle Solutions at 5°C

NiPAM:BAM	I_1/I_3
no particles	0.62 ± 0.01
100:0	0.73 ± 0.01
85:15	0.75 ± 0.06
65:35	0.81 ± 0.01
50:50	0.83 ± 0.01

by pyrene fluorescence analysis (Table 2),[38,39] which indicates that the particles provide a more hydrophobic environment than water. The ratio between the intensities of the first and third vibronic peaks in the fluorescence emission spectrum of pyrene is very sensitive to the polarity of the pyrene local environment. This probe has been used to monitor the polarity in solvents and colloidal aggregates.[38,39] The ratio increases with decreasing polarity of the surroundings. Table 2 shows the values of the I_1/I_3 ratio for the nanoparticles studied here. The values for the particles range from 0.73 for 100:0 to 0.83 for 50:50 NiPAM:BAM particles, all of which are higher than the value in water (0.62). This suggests that the particles provide a more hydrophobic environment than water, with a polarity similar to tetrahydrofuran or methanol. Moreover, the ratio, and consequently the hydrophobicity, increases as the percentage of BAM in the copolymeric nanoparticles increases. Accordingly, the pure NiPAM particles are the most hydrophilic and the 50:50 NiPAM:BAM particles the most hydrophobic of the series. The hydrophobicity gradually increases as the amount of BAM in the particles increases; thus, hydrophobicity cannot be the only source of attraction, and a second attractive interaction must play a role in binding and/or fibrillation inhibition.

Hydrogen bonding may occur between polar groups of the particle polymer backbone and polar groups of the peptide backbone and side chains. Alternatively, water molecules may hydrogen bond to both particle and protein. Hydrogen bonding between β strands is one of the structural features of protofilaments and fibrils.[40−44] Previous studies have shown that use of N-methylation to block the ability to form intermolecular H bonds prevents fibril elongation.[45−48] It is known that increasing the BAM content in NiPAM:BAM copolymeric composites decreases their H-bonding ability.[49] The higher inhibitory effect of the 100% NiPAM particles may thus be due to the formation of a larger number of H bonds on the surface, hindering the formation of critical nuclei and elongation of the fibril, with this inhibitory effect being reduced as the H-bonding capacity of the particles decreases with increasing BAM content in the particles.

Conclusions

We have shown that nanoparticles with a specific surface chemistry are capable of not just quenching but actually temporarily reversing the fibrillation of Aβ protein. While it has been possible to associate this phenomenon with binding of protein to the nanoparticles, the key steps may be monomer depletion (and subsequent shifting of the fibril equilibrium toward monomer) and/or trapping of sub- and near-critical nuclei (and subsequent kinetic blocking until the surface is saturated). Our findings may stimulate further experiments to elucidate the molecular details of the nanoparticle effect and enhance our understanding of the fibrillation process. The present studies were performed using pure Aβ without competition from other proteins for binding to the nanoparticle surface, which are conditions quite unlike those in any realistic clinical situation. Still, our studies may open interesting directions for future studies of fibril-related diseases and for the discovery of agents that interfere with the fibrillation process.

Acknowledgment. Funding for this work came from EU FP6 NanoInteract (I.L., K.A.D., and S.L.), EU MC RTN CIPSNAC (C.C.-L.), EPA Ireland (F.Q.-P.), IRCSET (C.C.-L.), a Ministerio de Educación y Ciencia postdoctoral grant (C.C.-L.), the Swedish Research Council (S.L.), SFI Walton (S.L.), and Welcome Trust Grant 067660 (D.M.W.).

Supporting Information Available: Materials and Methods, including a detailed description of the production of Aβ(M1−40) (Figure S1), particle size determination (Table S1), thioflavin T assay for synthetic Aβ(1−40) and Aβ(1−42) (Figure S2), ThT time course parallel to the TEM time course experiment (Figure S3), TEM images of copolymeric particles at high concentration (Figure S4), and scattering data from particle solutions over the concentration, temperature, and time-scale ranges used in the fibrillation studies (Figure S5). This material is available free of charge via the Internet at http://pubs.acs.org.

JA8041806

(38) Zana, R.; In, M.; Levy, H.; Duportail, G. *Langmuir* **1997**, *13*, 5552–5557.
(39) Kalyanasundaram, K.; Thomas, J. K. *J. Am. Chem. Soc.* **1977**, *99*, 2039–2044.
(40) Luhrs, T.; Ritter, C.; Adrian, M.; Riek-Loher, D.; Bohrmann, B.; Doeli, H.; Schubert, D.; Riek, R. *Proc. Natl. Acad. Sci. U.S.A.* **2005**, *102*, 17342–17347.
(41) Makin, O. S.; Atkins, E.; Sikorski, P.; Johansson, J.; Serpell, L. C. *Proc. Natl. Acad. Sci. U.S.A.* **2005**, *102*, 315–320.
(42) Nelson, R.; Sawaya, M. R.; Balbirnie, M.; Madsen, A. O.; Riekel, C.; Grothe, R.; Eisenberg, D. *Nature* **2005**, *435*, 773–778.
(43) Saiki, M.; Honda, S.; Kawasaki, K.; Zhou, D. S.; Kaito, A.; Konakahara, T.; Morii, H. *J. Mol. Biol.* **2005**, *348*, 983–998.
(44) Serpell, L. C.; Blake, C. C. F.; Fraser, P. E. *Biochemistry* **2000**, *39*, 13269–13275.
(45) Gordon, D. J.; Sciarretta, K. L.; Meredith, S. C. *Biochemistry* **2001**, *40*, 8237–8245.
(46) Hughes, E.; Burke, R. M.; Doig, A. J. *J. Biol. Chem.* **2000**, *275*, 25109–25115.
(47) Gordon, D. J.; Tappe, R.; Meredith, S. C. *J. Pept. Res.* **2002**, *60*, 37–55.
(48) Kokkoni, N.; Stott, K.; Amijee, H.; Mason, J. M.; Doig, A. J. *Biochemistry* **2006**, *45*, 9906–9918.
(49) Lynch, I.; Blute, I. A.; Zhmud, B.; MacArtain, P.; Tosetto, M.; Allen, L. T.; Byrne, H. J.; Farrell, G. F.; Keenan, A. K.; Gallagher, W. M.; Dawson, K. A. *Chem. Mater.* **2005**, *17*, 3889–3898.